The Journal of Experimental Biology 203, 3603–3612 (2000)
Printed in Great Britain © The Company of Biologists Limited 2000
JEB3106

PROCESSES CONTRIBUTING TO METABOLIC DEPRESSION IN HEPATOPANCREAS CELLS FROM THE SNAIL *HELIX ASPERSA*

T. BISHOP* AND M. D. BRAND
MRC Dunn Human Nutrition Unit, Hills Road, Cambridge CB2 2XY, UK
*e-mail: tb@mrc-dunn.cam.ac.uk

Accepted 8 September; published on WWW 2 November 2000

Summary

Cells isolated from the hepatopancreas of the land snail *Helix aspersa* strongly depress respiration both immediately in response to lowered P_{O_2} (oxygen conformation) and, in the longer term, during aestivation. These phenomena were analysed by dividing cellular respiration into non-mitochondrial and mitochondrial respiration using the mitochondrial poisons myxothiazol, antimycin and azide. Non-mitochondrial respiration accounted for a surprisingly large proportion, 65±5 %, of cellular respiration in control cells at 70 % air saturation. Non-mitochondrial respiration decreased substantially as oxygen tension was lowered, but mitochondrial respiration did not, and the oxygen-conforming behaviour of the cells was due entirely to the oxygen-dependence of non-mitochondrial oxygen consumption. Non-mitochondrial respiration was still responsible for 45±2 % of cellular respiration at physiological oxygen tension. Mitochondrial respiration was further subdivided into respiration used to drive ATP turnover and respiration used to drive futile proton cycling across the mitochondrial inner membrane using the ATP synthase inhibitor oligomycin. At physiological oxygen tensions, 34±5 % of cellular respiration was used to drive ATP turnover and 22±4 % was used to drive proton cycling, echoing the metabolic inefficiency previously observed in liver cells from mammals, reptiles and amphibians. The respiration rate of hepatopancreas cells from aestivating snails was only 37 % of the control value. This was caused by proportional decreases in non-mitochondrial and mitochondrial respiration and in respiration to drive ATP turnover and to drive proton cycling. Thus, the fraction of cellular respiration devoted to different processes remained constant and the cellular energy balance was preserved in the hypometabolic state.

Key words: metabolic depression, *Helix aspersa*, hepatopancreas, isolated cells, non-mitochondrial respiration, mitochondrial respiration, proton leak, aestivation, oxygen conformation, oxyconformation, mollusc, land snail.

Introduction

During the hot and dry months of summer, many animals face death by dehydration. To survive, they must either evade desiccation by moving to a cooler place or endure the assault by minimising water loss. For example, land snails endure arid conditions by retracting into their shells and secreting a thick mucous membrane, or epiphragm, over the shell entrance (Barnhart, 1983). Although water loss is minimised this way, feeding is not possible without breaking the epiphragm, so snails must, in addition, depress their metabolic rate to conserve energy. This phenomenon of metabolic depression is termed aestivation and has been well studied in land snails (see Hand and Hardewig, 1996; Guppy and Withers, 1999). It provides an excellent model system because, unlike the metabolic depression in hibernation, osmobiosis or anhydrobiosis, it is not confounded by changes in temperature or water content.

Until recently, aestivation could be studied at the level of the whole organism or at the level of the isolated tissue. For example, in the land snail *Helix aspersa*, the whole animal depresses oxygen consumption to 16 % of the control value and the mantle tissue depresses oxygen consumption to 52 % of the control value (Pedler et al., 1996). Although metabolically depressed tissue is a less complex and therefore easier model system for study than whole organisms, isolated cells are really required if the biochemical basis of metabolic depression is to be understood.

The recent development of an isolated cell preparation from the hepatopancreas of *Helix aspersa* which retains most of the metabolic depression seen at the level of the aestivating animal (Guppy et al., 2000) provides an excellent system for studying the cellular basis of metabolic depression. Cells from aestivating *Helix aspersa* have respiration rates that are depressed to 33 % of control values when rates at the physiological P_{O_2} and pH of aestivating snails are compared with rates at the physiological P_{O_2} and pH of control active snails. There are two components to the metabolic depression: extrinsic and intrinsic. During aestivation, the P_{O_2} of the haemolymph decreases from 42 to 29 % air saturation and its

pH decreases from 7.8 to 7.3 (Pedler et al., 1996). These decreases in P_{O_2} and pH, which are extrinsic to the cell, cause some of the observed metabolic depression; the former effect is termed oxygen conformation. Most of the metabolic depression, however, is due to changes that are intrinsic to the cells and takes several days to be fully expressed.

The present study characterises the contributions of different metabolic processes to the metabolic depression seen during oxygen conformation and the metabolic depression seen during aestivation in hepatopancreas cells isolated from *Helix aspersa*. Traditionally, the approach to understanding the mechanisms of metabolic depression has been to investigate a process or enzyme that one might predict to be metabolically depressed. For example, some organisms have been found to decrease the activities of glycolytic enzymes such as pyruvate kinase and phosphofructokinase that are involved in ATP production (e.g. Whitwam and Storey, 1990; Brooks and Storey, 1990); other organisms decrease the rates of Na^+/K^+-ATPase and protein synthesis, which are ATP consumers (e.g. Buck and Hochachka, 1993; Land et al., 1993; Krumschnabel et al., 1996). If metabolic depression is to occur whilst retaining homeostasis of intermediates such as ATP, however, multiple enzymes or processes need to be down-regulated during metabolic depression. It is unlikely that one could predict the full range of processes that may play a part, however small, in total reduction in metabolic rate. Comparisons between published data on various model systems might allow a greater range of target enzymes to be identified, but the problem then is one of universality of mechanisms of metabolic depression, i.e. how feasible is it to collate effects in different organisms due to different stresses?

In this study, a more holistic approach is taken to characterising metabolic depression. This is achieved by dividing the whole of metabolism into a small number of modules, or blocks of reactions, then comparing the fluxes through these blocks between control and metabolically depressed cells to determine which processes contribute to the observed changes in metabolic rate. As every enzyme that constitutes metabolism will lie in one of these blocks, every enzyme that plays a significant role in metabolic depression can be accounted for within one model system. Metabolism is divided into blocks on the basis of the natural divisions that exist in cells. We first divide oxidative metabolism into two major modules: mitochondrial respiration and non-mitochondrial respiration. These are distinguished by their sensitivity to specific inhibitors of mitochondrial electron transport, particularly myxothiazol, an inhibitor of complex III. We then subdivide mitochondrial respiration into respiration that is used to drive ATP synthesis and subsequent ATP turnover, and respiration that is not used for ATP turnover, but instead drives a futile cycle of proton pumping and leaking across the mitochondrial inner membrane. We distinguish these by their sensitivity to the specific inhibitor of the mitochondrial F_1F_o-ATP synthase, oligomycin. We show that the rate of non-mitochondrial respiration is surprisingly high, that it is responsible for the oxygen-conforming behaviour of the cells and that the metabolic depression seen during aestivation is caused by a proportional decrease in all the metabolic modules within the cells.

Materials and methods

Animals

Garden snails (*Helix aspersa* Müller), fresh mass approximately 7 g, were collected locally or bought from Blades Biological Systems (Kent, UK). They were washed and given water, lettuce and carrot mix (containing carrots, bran, milk powder and calcium carbonate) three times a week as described by Guppy et al. (2000). Snails were kept in plastic tanks in a Sanyo versatile environmental test chamber (MLR-350HT) maintained at 25 °C, 90 % relative humidity, under 120 W fluorescent light and on a 14 h:10 h L:D cycle starting at 09:00 h. After 2 weeks, half the snails were maintained as before and half were placed under the same conditions but without food or water and at 30 % relative humidity; after a further 16 days, these snails were fully aestivating (Guppy et al., 2000) and were used in this state for up to 2 months.

Isolation of hepatopancreas cells

Cells were isolated at 20–25 °C from active or aestivating *Helix aspersa*, as described by Guppy et al. (2000), using mechanical disruption and collagenase digestion of the hepatopancreas, followed by differential centrifugation in Sorvall SS-34 and MSE bench centrifuges. They were resuspended in incubation medium (10 mmol l^{-1} Hepes, 90 mmol l^{-1} NaCl, 5 mmol l^{-1} KCl, 5 mmol l^{-1} NaH_2PO_4, 2 mmol l^{-1} $MgCl_2$, 1 mmol l^{-1} $CaCl_2$, 5 mmol l^{-1} glucose, 1 mmol l^{-1} acetate, 10 mg ml^{-1} bovine serum albumin and 20 μg ml^{-1} gentamycin, at pH 7.8 or 7.3 as appropriate) and used within 3–4 h.

Isolation of hepatopancreas mitochondria

Isolation of hepatopancreas mitochondria was based on previous methods for mammalian tissues (Chappell and Hansford, 1972). All steps were carried out at 4 °C. The hepatopancreas was taken from 10 active or 10 aestivating snails, placed in isolation medium (250 mmol l^{-1} sucrose, 5 mmol l^{-1} Tris-HCl, 2 mmol l^{-1} EGTA, pH 7.4 at 4 °C), homogenised by 10 passes of a medium pestle in a 150 ml Wesley Coe glass homogeniser, and centrifuged for 3 min at 1050 ***g*** (Sorvall SS-34). The supernatant was centrifuged for 10 min at 11 600 ***g***, and the pellet was resuspended in fresh isolation medium. This centrifugation step was repeated twice, and the final pellet was resuspended in fresh isolation medium to a protein concentration of approximately 15 mg ml^{-1}.

Measurement of respiration rates

Respiration rates were measured using two 0.5 ml Clark oxygen electrodes (Rank Brothers, Bottisham, Cambridge, UK) thermostatted at 25 °C and connected to a Kipp & Zonen dual-channel chart recorder, assuming 479 nmol O ml^{-1} at air saturation (Reynafarje et al., 1985). Cell respiration rates were

expressed as a function of cell number, determined by an average of 10 counts (each of 50–100 cells) in 0.1 % (w/v) Neutral Red in an improved Neubauer haemocytometer. Respiration rates of isolated mitochondria were expressed per milligram protein, determined by biuret assay in the presence of sodium deoxycholate to disrupt membranes, using bovine serum albumin as a standard (Gornall et al., 1949). Mitochondria were diluted with assay medium (120 mmol l^{-1} KCl, 5 mmol l^{-1} KH_2PO_4, 3 mmol l^{-1} Hepes, 1 mmol l^{-1} EGTA, pH 7.2 at 25 °C) to 2.6 mg protein ml^{-1} in a 2 ml Clark electrode at 25 °C.

Cellular respiration rates depended on oxygen concentration, so protocols were designed to allow comparison of rates at the same oxygen concentration. Time courses of inhibition (see Figs 1A, 2A) were determined by adding 2 µl of inhibitor (in dimethylsulphoxide, DMSO) to cells in one electrode to give a final concentration of 2.5 µmol l^{-1} myxothiazol or 2 µg oligomycin per 10^6 cells, and 2 µl of DMSO simultaneously to cells in the other electrode, at different times before measuring respiration rates at 70 % air saturation. Concentration dependencies (see Figs 1B, 2B) were measured by adding 2 µl of myxothiazol or oligomycin at different concentrations to one electrode, and 2 µl of DMSO to the other electrode, at least 3 min before measuring respiration rates at 70 % air saturation. For other inhibitors (see Table 1), the times and concentrations used gave maximal inhibition (not shown). The extent of inhibition was calculated from the difference between the inhibited rate and the control rate. For the experiments to determine the inhibition conditions (see Figs 1, 2; Table 1), cells from active snails at pH 7.8 were diluted in the electrode with incubation medium to 4×10^6 cells ml^{-1}, and all measurements were made at 70 % air saturation. For the experiments to assay process rates (see Figs 3–5), cells were diluted in the electrode with incubation medium to 8×10^6 cells ml^{-1}.

Maximal inhibition by myxothiazol in isolated hepatopancreas mitochondria (which do not oxygen-conform; Guppy et al., 2000) was achieved by adding 3.6 µmol l^{-1} myxothiazol (in DMSO) to mitochondria uncoupled by 3.5 µmol l^{-1} carbonyl cyanide p-(trifluoromethoxy)phenyl-hydrazone (FCCP), in the presence of 7 µmol l^{-1} rotenone and 15 mmol l^{-1} potassium succinate.

The mechanisms of metabolic depression during oxygen conformation and aestivation (see Figs 3–5) were investigated using cells from active or aestivating snails at pH 7.8 or 7.3 at 8×10^6 cells ml^{-1}. Inhibitor (2 µl) was added to one electrode to give a final concentration of 5 µmol l^{-1} myxothiazol or 2 µg oligomycin per 10^6 cells, and 2 µl of DMSO was added to the other electrode. Respiration rates were measured after at least 3 min.

At any given oxygen tension, respiration insensitive to myxothiazol was defined as non-mitochondrial and respiration sensitive to myxothiazol (control rate minus rate in the presence of myxothiazol) was defined as mitochondrial. Similarly, at any given oxygen tension, respiration sensitive to oligomycin (control rate minus rate in the presence of oligomycin) was defined as respiration to drive ATP turnover, and respiration insensitive to oligomycin but sensitive to myxothiazol (rate in the presence of oligomycin minus rate in the presence of myxothiazol) was defined as respiration to drive proton leak. This assay for proton leak (effectively a measurement of the state 4 rate within the cells) measures proton leak rate after ATP turnover has been inhibited by oligomycin. Proton leak rate depends on proton-motive force, so this estimate will be an overestimate of the proton leak rate without oligomycin because of the increase in proton-motive force when oligomycin is added.

Statistical analyses

The average percentage depressions of different processes were calculated by dividing the average depressed value by the average control value. Differences between active and aestivating snail cell rates at physiological oxygen tensions and pH (see Fig. 4) were analysed using an unpaired *t*-test. A three-way analysis of variance (ANOVA) with P_{O_2} (42 % or 29 % air saturation), pH (7.8 or 7.3) and state (active or aestivating) as independent variables was then used to separate the effects of P_{O_2}, pH and state. The percentage contribution of each process to cellular respiration rate from active and aestivating snails at physiological oxygen tensions and pH (see Fig. 5) was calculated from individual daily percentages and analysed using a Mann–Whitney *U*-test. Statistical analyses were performed using StatView 5.0 (SAS Institute Inc.); *P* values below 0.05 were considered to be significant. Values are presented as means ± S.E.M.

Results

Inhibition conditions

The assays for non-mitochondrial and mitochondrial respiration, and of respiration to drive ATP turnover and proton cycling, required that inhibition by myxothiazol and oligomycin was complete, so the time course and concentration-dependence were measured for each inhibitor.

Myxothiazol maximally inhibited cellular respiration rate to 65±5 % of the control value after 3 min (Fig. 1A). A myxothiazol concentration of 1 µmol l^{-1} was required for maximal effect (Fig. 1B). Oligomycin maximally inhibited cellular respiration rate to 76±3 % of the control value after 3 min (Fig. 2A). A concentration of 1 µg oligomycin per 10^6 cells was required for maximal effect (Fig. 2B). Respiration rates were measured at 70 % air saturation, using cells from active snails. Inhibition time course and concentration-dependence did not differ in cells from aestivating snails (not shown).

It was surprising that myxothiazol inhibited respiration by only approximately 35 %. This raised doubt about the use of myxothiazol to distinguish mitochondrial from non-mitochondrial respiration. Isolated hepatopancreas mitochondria were used to test whether myxothiazol could completely inhibit complex III in *H. aspersa*. Respiration was inhibited to approximately 15 % of the control value (*N*=3),

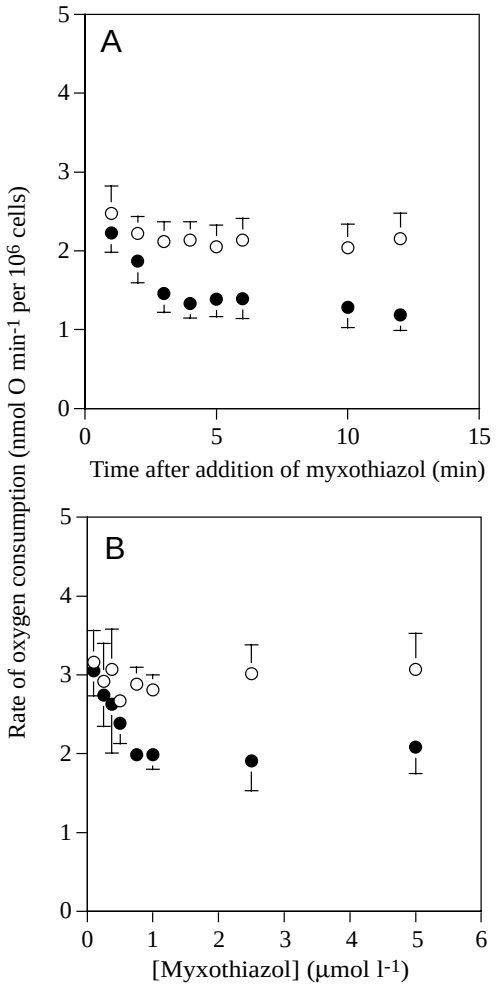

Fig. 1. (A) Time course and (B) concentration-dependence of myxothiazol inhibition of oxygen consumption in *Helix aspersa* hepatopancreas cells. Cells prepared from active snails and suspended in incubation medium at pH 7.8 were treated with myxothiazol as described in Materials and methods. Respiration rates were measured at 70 % air saturation. Values are means ± S.E.M., *N*=5 (A) or 6 (B). Open circles, control (DMSO only); filled circles, inhibited with myxothiazol (in DMSO).

showing that complex III in *H. aspersa* is indeed sensitive to myxothiazol. Antimycin, another inhibitor of complex III, inhibited cellular respiration to a similar extent as myxothiazol (Table 1), supporting the conclusion that non-mitochondrial oxygen consumption dominates cellular respiration. To test whether weak inhibition by complex III inhibitors is because electrons feed into the respiratory chain after complex III in *H. aspersa* hepatopancreas cells, inhibitors of complex IV were used (Table 1). Cyanide inhibited cellular respiration to 35±5 % of the control value, which is significantly greater inhibition than with inhibitors of complex III. Cyanide, however, is relatively unspecific (Yonetani, 1976), so it is possible that this greater inhibition was due to partial cyanide inhibition of non-mitochondrial respiration. This suggestion is supported by the observation that another inhibitor of complex IV, azide, inhibited cellular respiration rate to a similar extent as myxothiazol (to 75 % of the control value; Table 1). Finally, bacteria, which are typically myxothiazol-insensitive, might have accounted for a large proportion of respiration in the cell preparations, making it mostly myxothiazol-insensitive. The cell suspension was filtered through a 5 μm pore nitrocellulose filter, which retains cells (not less than approximately 13 μm in diameter; Guppy et al., 2000) but not bacteria. The respiration rate of the filtrate was less than 10 % of the total cellular rate at 70 % air saturation. Contamination of the cell preparation by bacteria was therefore small, as found previously by Guppy et al. (2000). Hepatopancreas cells were salicylhydroxamic acid (SHAM)-insensitive (Table 1), suggesting that the non-mitochondrial oxygen consumption does not involve a plant-like alternative oxidase.

Table 1. *Inhibition of oxygen consumption in* Helix aspersa *hepatopancreas cells*

Inhibitor (site of action)	Respiration rate after inhibition (% of control)	*N*
Rotenone (complex I)	100	1
Myxothiazol (complex III)	64±2	11
Antimycin A (complex III)	73±4	5
Potassium cyanide (complex IV)	35±5	4
Sodium azide (complex IV)	75	1
SHAM (alternative oxidase)	100	2

Cells from active snails were suspended in incubation medium at pH 7.8, 25 °C. Inhibitor (up to 0.2 mmol l^{-1} rotenone, dissolved in ethanol; 2.5 μmol l^{-1} myxothiazol, 2.5 μmol l^{-1} antimycin or up to 0.2 mmol l^{-1} salicylhydroxamic acid (SHAM), dissolved in dimethylsulphoxide (DMSO); 3 mmol l^{-1} potassium cyanide or 3 mmol l^{-1} sodium azide dissolved in 0.5 mol l^{-1} Hepes at pH 7.8) was added to one electrode (these concentrations are known to cause maximal inhibition), and the same volume of the appropriate solvent was added to a parallel, control electrode. Inhibitors were added at least 3 min before respiration rates were measured, at 70 % air saturation. The control respiration rate was 3.04±0.95 nmol O min^{-1} per 10^6 cells.

Values are mean ± S.E.M. of *N* independent replicates.

In summary, therefore, the modest inhibition of cellular respiration with myxothiazol was not artefactually low. This means that non-mitochondrial respiration accounted for a large proportion of the total cellular rate. Myxothiazol and oligomycin were therefore used, under conditions known to cause maximal inhibition, to subdivide cellular respiration in subsequent experiments.

Metabolic depression during oxygen conformation

As shown by Guppy et al. (2000), cells from aestivating snails incubated at pH 7.3 had significantly lower respiration rates at all oxygen tensions than cells from active snails incubated at pH 7.8 (Fig. 3A). Moreover, cells from both active and aestivating snails showed oxygen-conforming behaviour,

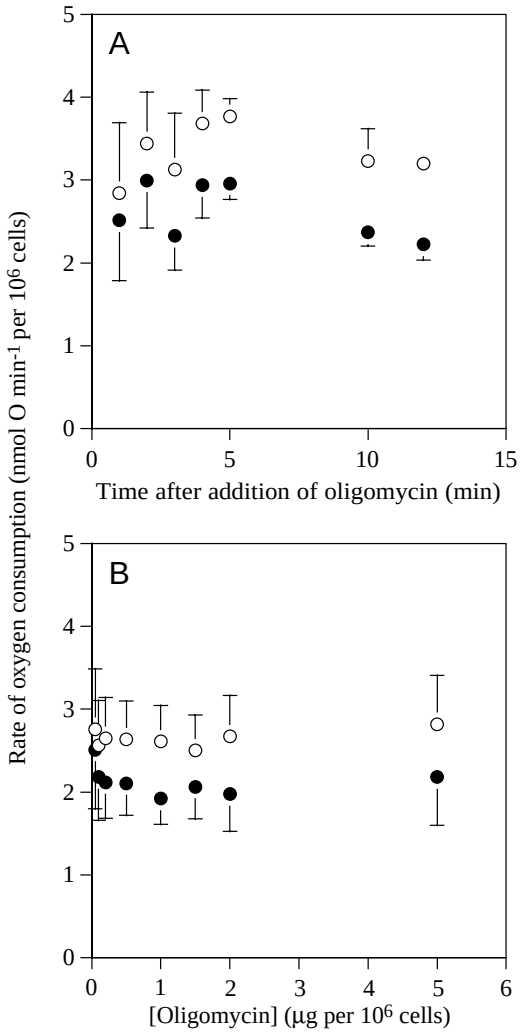

Fig. 2. (A) Time course and (B) concentration-dependence of oligomycin inhibition of oxygen consumption in *Helix aspersa* hepatopancreas cells. Cells prepared from active snails and suspended in incubation medium at pH 7.8 were treated with oligomycin as described in Materials and methods. Respiration rates were measured at 70 % air saturation. Values are means ± S.E.M., *N*=4 (A) or 5 (B). Open circles, control (DMSO only); filled circles, inhibited with oligomycin (in DMSO).

i.e. respiration rate decreased with decreasing oxygen tension across the whole range of oxygen tensions.

What oxygen consumer is responsible for this oxygen conformation? Non-mitochondrial respiration followed the same trend as the overall cellular rate: as oxygen tension decreased, respiration rate decreased (Fig. 3B). In contrast, mitochondrial respiration rate did not decrease with decreasing oxygen tension (Fig. 3C). (The apparent decrease in mitochondrial respiration of cells from active snails at pH 7.8 at high, unphysiological oxygen tensions is probably a small measurement artefact linked to equilibration of the cells when they were placed in the electrode). Similarly, respiration to drive proton cycling did not decrease with decreasing oxygen tension (Fig. 3D). In cells from active snails at physiological oxygen tension and pH, non-mitochondrial respiration accounted for 45±2 % of cellular respiration, ATP turnover accounted for 34±5 % and proton cycling accounted for 22±4 % (see Fig. 5).

In summary, oxygen conformation in *H. aspersa* hepatopancreas cells from both active and aestivating snails was due to decreased non-mitochondrial respiration only. Mitochondrial respiration remained constant with changing P_{O_2}. Consumption of oxygen to drive mitochondrial proton cycling was a significant proportion of cellular respiration rate and remained constant with changing P_{O_2}. Because of decreased non-mitochondrial respiration, overall metabolic efficiency increased considerably as oxygen tension decreased.

Metabolic depression during aestivation

The average respiration rates of cells from aestivating snails at their physiological P_{O_2} and pH (point *d*, Fig. 4A) were depressed to 37±6 % of the respiration rates of cells from active snails at their physiological P_{O_2} and pH (point *a*, Fig. 4A; $P<0.0001$). The decrease in P_{O_2} from 42 % to 29 % air saturation (point *a* to point *b*, Fig. 4A; $P<0.001$) and change in state from active to aestivating (point *c* to point *d*, Fig. 4A; $P<0.0001$) each resulted in a significant metabolic depression. This agrees with the results of Guppy et al. (2000). The decrease in pH from 7.8 to 7.3 (point *b* to point *c*, Fig. 4A), however, did not result in a significant metabolic depression.

During aestivation, non-mitochondrial respiration decreased to 36±6 % of the control value when cells from active and aestivating snails were compared at their physiological P_{O_2} and pH (point *a* to point *d*, Fig. 4B; $P<0.0001$). The decrease in P_{O_2} (point *a* to point *b*, Fig. 4B; $P<0.0001$) and the change in state (point *c* to point *d*, Fig. 4B; $P<0.0001$) each caused a significant decrease in non-mitochondrial respiration; the decrease in pH (point *b* to point *c*, Fig. 4B), however, did not.

Mitochondrial respiration also decreased during aestivation, to 38±10 % of the control value, when cells from active and aestivating snails were compared at their physiological P_{O_2} and pH (point *a* to point *d*, Fig. 4C; $P<0.001$). The decrease in pH (point *b* to point *c*, Fig. 4C; $P<0.05$) and the change in state (point *c* to point *d*, Fig. 4C; $P<0.0001$) each caused a significant decrease in mitochondrial respiration; the decrease in P_{O_2} (point *a* to point *b*, Fig. 4C), however, did not.

Proton cycling followed a similar pattern to mitochondrial respiration. It decreased to 26±12 % of the control value during aestivation when cells from active and aestivating snails were compared at their physiological P_{O_2} and pH (point *a* to point *d*, Fig. 4D; $P<0.01$). The decrease in pH (point *b* to point *c*, Fig. 4D; $P<0.05$) and the change in state (point *c* to point *d*, Fig. 4D; $P<0.01$) each caused a significant decrease in proton leak respiration; the decrease in P_{O_2} (point *a* to point *b*, Fig. 4D), however, did not.

These results are summarised in Fig. 5A,B. The respiration of cells from active snails at their physiological P_{O_2} and pH was 45 % non-mitochondrial and 55 % mitochondrial. Within mitochondrial respiration, 34 % of cellular respiration was used

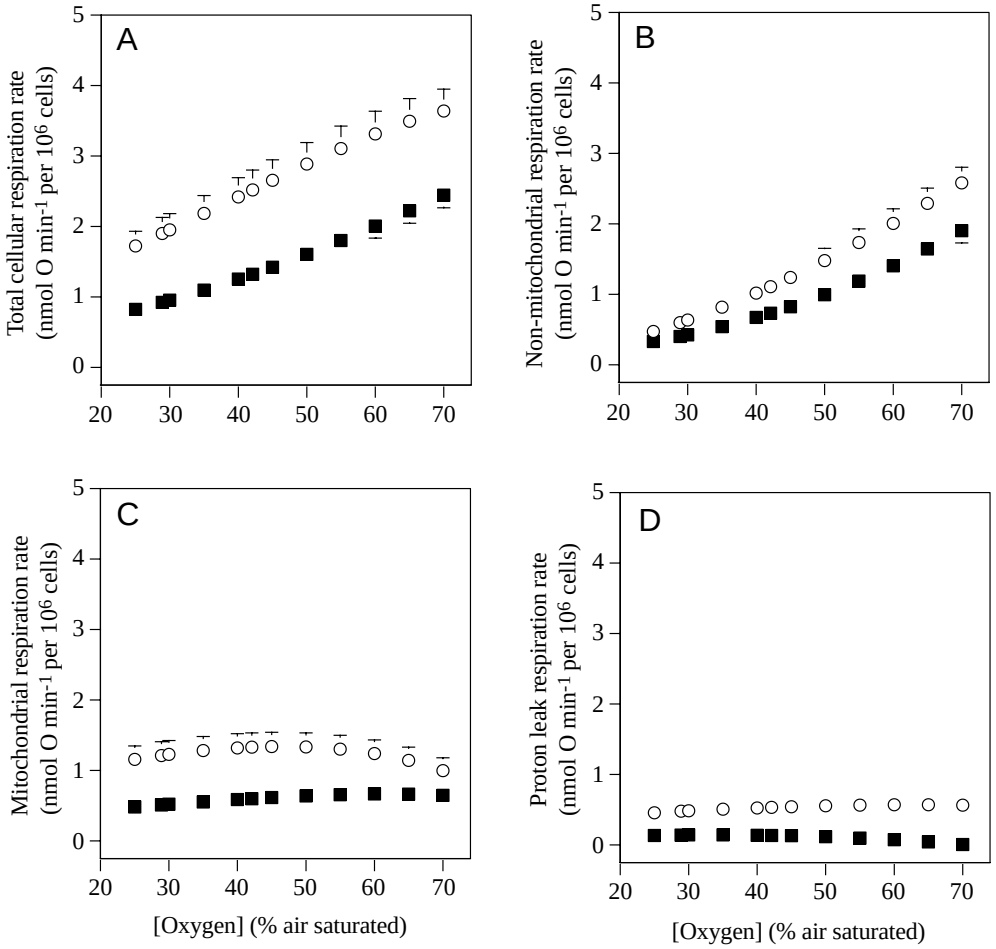

Fig. 3. Processes contributing to the respiration rate of hepatopancreas cells from active and aestivating *Helix aspersa*. (A) Total cellular respiration, (B) non-mitochondrial respiration (oxygen consumption in the presence of myxothiazol), (C) mitochondrial respiration (oxygen consumption sensitive to myxothiazol), (D) respiration to drive mitochondrial proton cycling (oxygen consumption in the presence of oligomycin minus oxygen consumption in the presence of myxothiazol). Cells prepared from active or aestivating snails were suspended in parallel in incubation buffer at pH 7.8 or pH 7.3, respectively, and treated with myxothiazol or oligomycin as described in Materials and methods. Respiration rates were measured at the oxygen tensions indicated as the cells progressively removed oxygen from the medium. Values are means ± S.E.M. (N=9). Open circles, active, pH 7.8; filled squares, aestivating, pH 7.3.

to drive ATP turnover and 22 % was for proton cycling. During aestivation, when P_{O_2} and pH decrease and the cells change state, total cellular respiration rate dropped to 37 % of the respiration rate of cells from active snails. Although non-mitochondrial and mitochondrial respiration, ATP turnover and proton cycling all decreased during aestivation, they did so to the same extent as the decrease in total cellular respiration. In cells from aestivating animals, 50±7 % of respiration was non-mitochondrial, 50±7 % was mitochondrial and, within mitochondrial respiration, 38±4 % was for ATP turnover and 12±7 % was for proton cycling (Fig. 5B). Therefore, each reaction accounted for a similar proportion of cellular respiration rate before and during aestivation, and the active pattern of energy expenditure was maintained, but at a lower intensity, during aestivation.

The maintenance of the relative proportions of different processes is especially interesting with regards to proton leak. If cells were to depress their metabolic rate to 37 % of the control value without changing proton leak rate, then proton cycling, which accounts for 22 % of respiration in cells from active snails, would dominate the cellular respiration rate during aestivation, decreasing metabolic efficiency. Our finding that proton leak rate is depressed during aestivation shows that the metabolic efficiency of the cell is at least conserved and may even be increased.

Discussion

This study demonstrates for the first time the subcellular basis for metabolic depression in an isolated cell system: hepatopancreas cells from *Helix aspersa*. Non-mitochondrial respiration in these cells is a surprisingly high proportion of total respiration, and its dependence on oxygen concentration completely explains the marked oxygen-conforming behaviour of the cells. The decrease in non-mitochondrial respiration at lower oxygen tensions results in increased metabolic efficiency (i.e. more ATP synthesis per oxygen consumed). The strong depression of respiration caused by aestivation is explained by proportional decreases in non-mitochondrial and mitochondrial oxygen consumption. Within mitochondrial respiration, ATP turnover and mitochondrial proton cycling also decreased in proportion so that, overall, the pattern of oxygen consumption and the metabolic efficiency are maintained during the hypometabolic state.

Relative contributions of different biochemical processes to cellular respiration

In control cells from active snails at their physiological P_{O_2} and pH, 45 % of oxygen consumption was non-mitochondrial and 55 % was mitochondrial. Within mitochondrial respiration, 34 % was used to drive ATP turnover and 22 % to drive proton

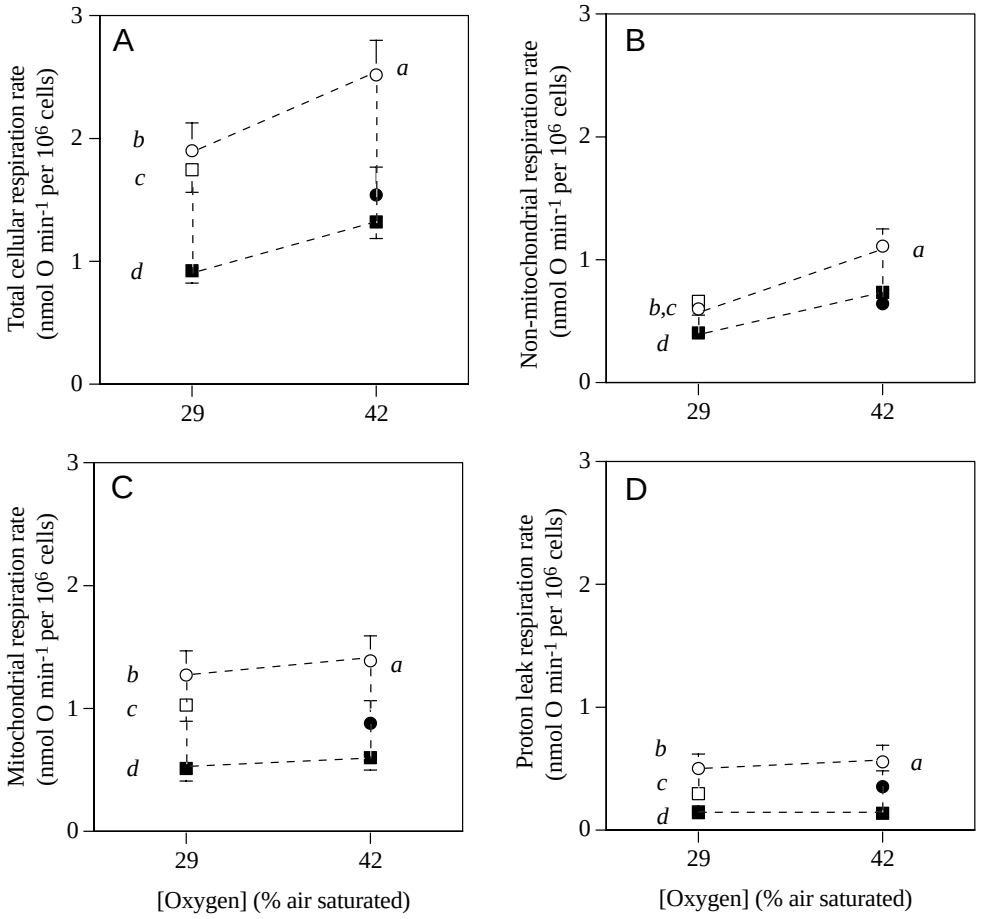

Fig. 4. Processes contributing to the respiration rate of hepatopancreas cells from active and aestivating *Helix aspersa* at physiological oxygen tensions. (A) Total cellular respiration, (B) non-mitochondrial respiration (oxygen consumption in the presence of myxothiazol), (C) mitochondrial respiration (oxygen consumption sensitive to myxothiazol), (D) respiration to drive mitochondrial proton cycling (oxygen consumption in the presence of oligomycin minus oxygen consumption in the presence of myxothiazol). Data are from Fig. 3 and for cells from active snails incubated at pH 7.3, at 42 % and 29 % air saturation only (the physiological oxygen tensions for cells from active and aestivating snails, respectively). Dotted lines represent the progression into metabolic depression from active, 42 % air saturation, pH 7.8, to aestivating, 29 % air saturation, pH 7.3, as a result of changes in P_{O_2}, pH and state, then the progression out of metabolic depression as a result of the reverse changes. Physiological active snail cells (P_{O_2} 42 % air saturation and pH 7.8) are at point *a*; a decrease in P_{O_2} gives active snail cells at P_{O_2} 29 % air saturation and pH 7.8 (point *b*); a decrease in pH gives active snail cells at P_{O_2} 29 % air saturation and pH 7.3 (point *c*); finally, a change in state from active to aestivating gives physiological aestivating snail cells (P_{O_2} 29 % air saturation and pH 7.3, point *d*). There are no significant interactions between P_{O_2}, pH and state; P_{O_2} has a significant effect on total cellular and non-mitochondrial respiration; pH has a significant effect on mitochondrial and proton leak respiration, and state has a significant effect on total cellular, non-mitochondrial, mitochondrial and proton leak respiration (three-way ANOVA). Respiration rates are means ± S.E.M., N=9 (active, pH 7.8 and aestivating, pH 7.3) and 10 (active, pH 7.3). Open circles, active, pH 7.8; open squares, active, pH 7.3; filled squares, aestivating, pH 7.3; filled circles, aestivating, pH 7.8.

cycling. It is surprising that non-mitochondrial respiration accounted for such a large proportion of cellular respiration. Only approximately 10–20 % of respiration rate in mammalian and fish cells is non-mitochondrial (Nobes et al., 1990; Rolfe and Brand, 1996; Rolfe et al., 1999; Savina and Gamper, 1998), although we are not aware of any estimates for invertebrates.

Enzymes that could account for this high non-mitochondrial oxygen uptake include those found within the endoplasmic reticulum and within peroxisomes (van den Bosch et al., 1992). For example, xanthine oxidase (Harrison, 1997) and cytochrome P450, both found in the endoplasmic reticulum, may be candidates. Similarly, the peroxisomal oxidases (urate oxidase, D-amino acid oxidase, L-α-hydroxyacid oxidase A and B, acyl-CoA oxidase and oxalate oxidase) may play a part. Alternatively, the high non-mitochondrial oxygen consumption may be due to enzymes specific to the hepatopancreas, a digestive organ that combines the roles of the liver and pancreas. Non-mitochondrial oxygen consumption might be a protective mechanism to remove oxygen when it is present at high, potentially damaging, concentrations: this could explain its strong oxygen-dependence.

It is also interesting that mitochondrial proton cycling accounts for approximately 20 % of the total cellular respiration rate. This is the first estimate of proton cycling in cells from an invertebrate, and it is similar to the values of 20–30 % of cellular respiration found in hepatocytes from a variety of vertebrates, both endothermic (Nobes et al., 1990; Brand et al., 1994; Porter and Brand, 1995; Rolfe et al., 1999) and ectothermic (Brand et al., 1991, 2000; Savina and Gamper, 1998). Despite the differences in cellular metabolism that exist between vertebrates and invertebrates, therefore, the amount of energy dissipated by proton cycling appears to be very similar, supporting the idea that it is not primarily for thermogenesis but that it fulfils some other very important and widespread function, such as protection against oxidative damage (Skulachev, 1996; Brand, 2000).

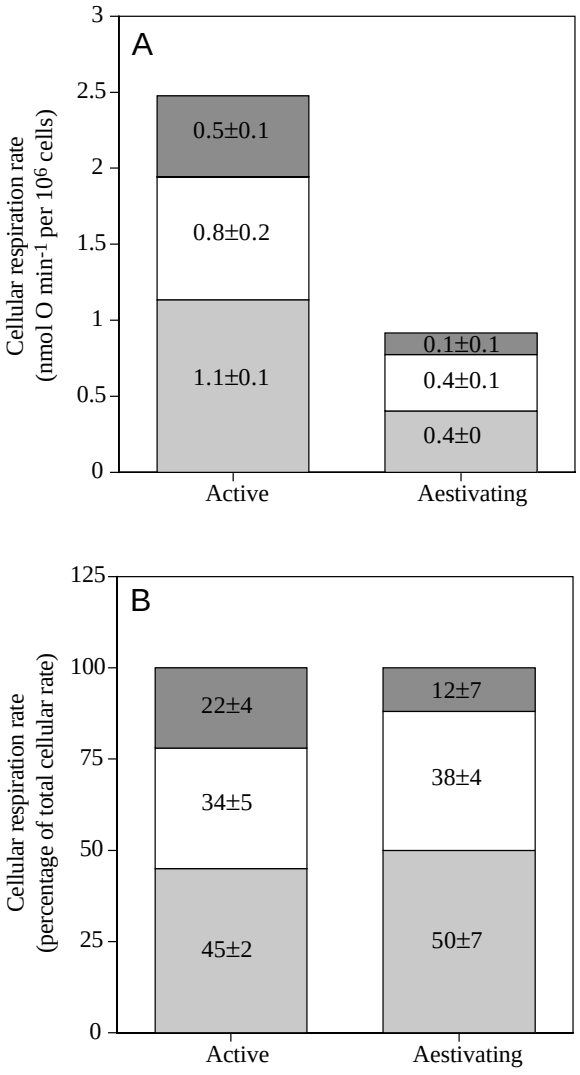

Fig. 5. Processes contributing to the respiration rate of hepatopancreas cells from active and aestivating *Helix aspersa* at their physiological oxygen tension and pH. (A) Absolute rates; (B) rates expressed as a percentage of the total for that condition. Non-mitochondrial respiration, mitochondrial respiration and respiration to drive mitochondrial proton cycling are from Fig. 4 and are shown for cells isolated from active snails incubated at their physiological oxygen tension (P_{O_2} 42 % air saturation) and pH (7.8) and for cells isolated from aestivating snails incubated at their physiological oxygen tension (P_{O_2} 29 % air saturation) and pH (7.3). There are no significant differences between the percentage contributions of non-mitochondrial and mitochondrial respiration, or respiration to drive ATP turnover and proton leak of cells from active and aestivating snails (Mann–Whitney *U*-test). Dark grey columns, proton leak; white columns, ATP turnover; light grey columns, non-mitochondrial respiration.

Oxygen conformation

At lower oxygen concentrations, the non-mitochondrial respiration rate decreased, but mitochondrial respiration, including oxygen consumption to drive the mitochondrial proton cycle, remained constant. Oxygen conformation in these cells is therefore due entirely to the properties of non-mitochondrial respiration. This contrasts with the metabolic depression seen in response to hypoxia and anoxia in isolated goldfish (*Carassius auratus*) and turtle (*Chrysemys picta bellii*) hepatocytes, in which reactions linked to mitochondrial respiration such as rates of Na^+/K^+-ATPase and protein synthesis are reduced in the hypometabolic state (Krumschnabel et al., 1996; Buck and Hochachka, 1993; Land et al., 1993). Although a haem-based oxygen-sensing mechanism is involved in depression of turtle hepatocyte protein synthesis during anoxia (Land and Hochachka, 1995), it is unclear whether oxygen conformation in *Helix aspersa* cells also involves oxygen sensing (for a review, see Bunn and Poyton, 1996).

Aestivation

The metabolic depression of snail hepatopancreas cells during aestivation was caused by proportional decreases in non-mitochondrial and mitochondrial respiration and in the components of mitochondrial respiration, ATP turnover and proton cycling. Non-mitochondrial respiration decreased in response to decreased P_{O_2} (oxygen conformation) as well as in response to changed state. Mitochondrial respiration and proton leak decreased in response to decreased pH and changed state. The rate of each process decreased to the same extent as the overall metabolic depression, so that they accounted for similar proportions of cellular respiration rate before and during aestivation. It should be noted that these were acute responses to changes in P_{O_2} and pH, and that long-term adaptational responses may be different.

Most theories surrounding mechanisms of aerobic metabolic depression invoke down-regulation of enzymes and processes linked to mitochondrial respiration. For example, reductions in the activities of enzymes involved in ATP-producing processes, such as carbohydrate degradation, have been reported, as have reductions in ATP-consuming processes (for reviews, see Guppy and Withers, 1999; Hand and Hardewig, 1996). In *H. aspersa* cells, mitochondrial respiration does decrease during aestivation, but so does non-mitochondrial respiration.

ATP consumption in mammalian cells is responsible for approximately 70 % of respiration, which is dedicated approximately 20 % to protein synthesis and breakdown, 20 % to Na^+ cycling, 5 % to Ca^{2+} cycling, 5 % to gluconeogenesis and glycolysis, 5 % to actinomyosin contraction/relaxation, 2 % to ureagenesis and the remaining 10–15 % to mRNA synthesis, substrate cycling and other unquantified reactions (Rolfe and Brand, 1996; Rolfe et al., 1999; for a review, see Rolfe and Brown, 1997). Among these energy-consuming processes, the rates of protein synthesis and the activity of the Na^+/K^+-ATPase are reduced in many different metabolically depressed animals (for a review, see Guppy and Withers, 1999). Similarly, the ATP demand for protein synthesis, protein breakdown, ureagenesis, gluconeogenesis and the Na^+/K^+-ATPase were shown to be reduced when normoxic turtle hepatocytes were exposed to anoxia (for a review, see

Hochachka et al., 1997). The finding that ATP turnover decreased during aestivation in *Helix aspersa* hepatopancreas cells therefore agrees with the results of these studies.

Few studies exist that examine the possibility that mitochondrial proton cycling is down-regulated during metabolic depression. Yet, proton cycling makes up a substantial proportion of metabolic rate in many different animals, perhaps 20–30 % (Brand et al., 1994, 2000; Stuart et al., 1999a). Animals that depress their metabolic rate to 20 % need, therefore, to decrease their proton leak rate very strongly or most of the reduced metabolic rate would be devoted to dissipating energy through proton leak. Here, we find that proton leak is indeed decreased during aestivation so that energetic efficiency is at least conserved and may even be increased. This is in agreement with studies carried out on isolated muscle mitochondria from the overwintering frog *Rana temporaria*, in which the proton leak rate was found to be decreased compared with that of control frogs (St. Pierre et al., 2000).

There are three ways in which proton cycling rate in cells may be decreased (see Brand, 1990). (i) The area of mitochondrial inner membrane can be decreased, so that there is less surface across which proton leak can occur. An example of this occurs in hepatocytes of larger mammals, mostly by a decrease in the volume density of the mitochondria within the cells (Porter et al., 1996). (ii) The activity of the block of reactions that catalyse substrate oxidation can be decreased, so that there is less driving force for proton leak. This is seen in mitochondria from toads (*Xenopus laevis laevis* and *Bufo marinus*) (Brookes et al., 1998) and frogs (*Rana temporaria*) (St. Pierre et al., 2000). (iii) The proton conductance of the mitochondrial inner membrane can be decreased, so that the proton leak rate across a given area of membrane is decreased at any given driving force. An example of this is the decreased proton conductance of mitochondria in hepatocytes from hypothyroid rats (Brand et al., 1992; Harper and Brand, 1993).

The decreased proton leak rate in muscle mitochondria from hibernating frogs was due to decreased substrate oxidation activity and did not involve a decrease in the proton conductance (St. Pierre et al., 2000), showing that mechanism *ii* can be involved in metabolic depression. In the aestivating land snail *Cepaea nemoralis*, however, phospholipid fatty acyl composition was altered in a way suggestive of decreased proton conductance (Stuart et al., 1999b), in line with mechanism *iii*. Further studies will elucidate the mechanisms of decreased proton cycling in hepatopancreas cells from aestivating *H. aspersa*.

We thank Julie St. Pierre and Jeff Stuart for their advice, and the Medical Research Council (M.D.B.), Trinity Hall and Cambridge Commonwealth Trust (T.B.) for financial support.

References

Barnhart, M. C. (1983). Gas permeability of the epiphragm of a terrestrial snail, *Otala lactea*. *Physiol. Zool.* **56**, 436–444.

Brand, M. D. (1990). The contribution of the leak of protons across the mitochondrial inner membrane to standard metabolic rate. *J. Theor. Biol.* **145**, 267–286.

Brand, M. D. (2000). Uncoupling to survive? The role of mitochondrial inefficiency in ageing. *Exp. Gerontol.* (in press).

Brand, M. D., Bishop, T., Boutilier, R. G. and St-Pierre, J. (2000). Mitochondrial proton conductance, standard metabolic rate and metabolic depression. In *Life in the Cold* (ed. G. Heldmaier and M. Klingenspor), pp. 413–430. Berlin, Heidelberg, New York: Springer.

Brand, M. D., Chien, L.-F., Ainscow, E. K., Rolfe, D. F. S. and Porter, R. K. (1994). The causes and functions of mitochondrial proton leak. *Biochim. Biophys. Acta* **1187**, 132–139.

Brand, M. D., Couture, P., Else, P. L., Wither, K. W. and Hulbert, A. J. (1991). Evolution of energy metabolism: proton permeability of the inner membrane of liver mitochondria is greater in a mammal than in a reptile. *Biochem. J.* **275**, 81–86.

Brand, M. D., Steverding, D., Kadenbach, B., Stevenson, P. M. and Hafner, R. P. (1992). The mechanism of the increase in mitochondrial proton permeability induced by thyroid hormones. *Eur. J. Biochem.* **206**, 775–781.

Brookes, P. S., Buckingham, J. A., Tenreiro, A. M., Hulbert, A. J. and Brand, M. D. (1998). The proton permeability of the inner membrane of liver mitochondria from ectothermic and endothermic vertebrates and from obese rats: correlations with standard metabolic rate and phospholipid fatty acid composition. *Comp. Biochem. Biophys.* **119**B, 325–334.

Brooks, S. P. J. and Storey, K. B. (1990). Glycolytic enzyme binding and metabolic control in estivation and anoxia in the land snail *Otala lactea*. *J. Exp. Biol.* **151**, 193–204.

Buck, L. T. and Hochachka, P. W. (1993). Anoxic suppression of Na^+–K^+-ATPase and constant membrane potential in hepatocytes: support for channel arrest. *Am. J. Physiol.* **265**, R1020–R1025.

Bunn, H. F. and Poyton, R. O. (1996). Oxygen sensing and molecular adaptation to hypoxia. *Physiol. Rev.* **76**, 839–885.

Chappell, J. B. and Hansford, R. G. (1972). Preparation of mitochondria from animal tissues and yeasts. In *Subcellular Components: Preparation and Fractionation*, second edition (ed. G. D. Birnie), pp. 77–91. London: Butterworth.

Gornall, A. G., Bardawill, C. J. and David, M. M. (1949). Determination of serum protein by means of the biuret reaction. *J. Biol. Chem.* **177**, 751–766.

Guppy, M., Reeves, D. C., Bishop, T., Withers, P., Buckingham, J. A. and Brand, M. D. (2000). Intrinsic metabolic depression in cells isolated from the hepatopancreas of estivating snails. *FASEB J.***14**, 999–1004.

Guppy, M. and Withers, P. (1999). Metabolic depression in animals: physiological perspectives and biochemical generalizations. *Biol. Rev.* **74**, 1–40.

Hand, S. C. and Hardewig, I. (1996). Downregulation of cellular metabolism during environmental stress: mechanisms and implications. *Annu. Rev. Physiol.* **58**, 539–563.

Harper, M.-E. and Brand, M. D. (1993). The quantitative contributions of mitochondrial proton leak and ATP turnover reactions to the changed respiration rates of hepatocytes from rats of different thyroid status. *J. Biol. Chem.* **268**, 14850–14860.

Harrison, R. (1997). Human xanthine oxidoreductase: in search of a function. *Biochem. Soc. Trans.* **25**, 786–791.

Hochachka, P. W., Land, S. C. and Buck, L. T. (1997). Oxygen sensing and signal transduction in metabolic defence against hypoxia: lessons from vertebrate facultative anaerobes. *Comp. Biochem. Physiol.* **118**A, 23–29.

Krumschnabel, G., Biasi, C., Schwarzbaum, P. J. and Wieser, W. (1996). Membrane–metabolic coupling and ion homeostasis in anoxia-tolerant and anoxia-intolerant hepatocytes. *Am. J. Physiol*. **270**, R614–R620.

Land, S. C., Buck, L. T. and Hochachka, P. W. (1993). Response of protein synthesis to anoxia and recovery in anoxia-tolerant hepatocytes. *Am. J. Physiol*. **265**, R41–R48.

Land, S. C. and Hochachka, P. W. (1995). A heme-protein-based oxygen-sensing mechanism controls the expression and suppression of multiple proteins in anoxia-tolerant turtle hepatocytes. *Proc. Natl. Acad. Sci. USA* **92**, 7505–7509.

Nobes, C. D., Brown, G. C., Olive, P. N. and Brand, M. D. (1990). Non-ohmic proton conductance of the mitochondrial inner membrane in hepatocytes. *J. Biol. Chem.* **265**, 12903–12909.

Pedler, S., Fuery, C. J., Withers, P. C., Flanigan, J. and Guppy, M. (1996). Effectors of metabolic depression in an estivating pulmonate snail (*Helix aspersa*): whole animal and *in vitro* tissue studies. *J. Comp. Physiol.* B **166**, 375–381.

Porter, R. K. and Brand, M. D. (1995). Causes of differences in respiration rate of hepatocytes from mammals of different body mass. *Am. J. Physiol*. **269**, R1213–R1224.

Porter, R. K., Hulbert, A. J. and Brand, M. D. (1996). Allometry of mitochondrial proton leak: influence of membrane surface area and fatty acid composition. *Am. J. Physiol*. **271**, R1550–R1560.

Reynafarje, B., Costa, L. and Lehninger, A. (1985). O_2 solubility in aqueous media determined by a kinetic method. *Analyt. Biochem*. **145**, 406–418.

Rolfe, D. F. S. and Brand, M. D. (1996). Contribution of mitochondrial proton leak to skeletal muscle respiration and to standard metabolic rate. *Am. J. Physiol*. **271**, C1380–C1389.

Rolfe, D. F. S. and Brown, G. C. (1997). Cellular energy utilisation and molecular origin of standard metabolic rate in mammals. *Physiol. Rev*. **77**, 731–758.

Rolfe, D. F. S., Newman, J. M. B., Buckingham, J. A., Clark, M. G. and Brand, M. D. (1999). Contribution of mitochondrial proton leak to respiration rate in working skeletal muscle and liver and to SMR. *Am. J. Physiol*. **276**, C692–C699.

Savina, M. V. and Gamper, N. L. (1998). Respiration and adenine nucleotides of Baltic lamprey (*Lampetra fluviatilis* L.) hepatocytes during spawning migration. *Comp. Biochem. Physiol.* **120** B, 375–383.

Skulachev, V. P. (1996). Role of uncoupled and non-coupled oxidations in maintenance of safely low levels of oxygen and its one-electron reductants. *Q. Rev. Biophys.* **29**, 169–202.

St. Pierre, J., Brand, M. D. and Boutilier, R. G. (2000). The effect of metabolic depression on proton leak rate in mitochondria from hibernating frogs. *J. Exp. Biol.* **203**, 1469–1476.

Stuart, J. A., Brindle, K. M., Harper, J. A. and Brand, M. D. (1999a). Mitochondrial proton leak and the uncoupling proteins. *J. Bioenerg. Biomembr*. **31**, 517–525.

Stuart, J. A., Gillis, T. E. and Ballantyne, J. S. (1999b). Compositional correlates of metabolic depression in the mitochondrial membranes of estivating snails, *Cepaea nemoralis*. *Am. J. Physiol.* **275**, 1977–1982.

van den Bosch, H., Schutgens, R. B. H., Wanders, R. J. A. and Tager, J. M. (1992). Biochemistry of peroxisomes. *Annu. Rev. Biochem*. **61**, 157–197.

Whitwam, R. E. and Storey, K. B. (1990). Pyruvate kinase from the land snail *Otala lactea*: regulation by reversible phosphorylation during estivation and anoxia. *J. Exp. Biol.* **154**, 321–337.

Yonetani, T. (1976). Cytochrome c peroxidase. In *The Enzymes*, vol. XIII, *Oxidation–Reduction*, part C (ed. P. D. Boyer), pp. 345–361. New York, London: Academic Press.